Published in final edited form as:

J Pharm Biomed Anal. 2021 May 10; 198: 113996. doi:10.1016/j.jpba.2021.113996.

The synthesis and characterization of Bri2 BRICHOS coated magnetic particles and their application to protein fishing: Identification of novel binding proteins

Helene Tigro[a], **Nina Kronqvist**[b], **Axel Abelein**[b], **Lorena Galan-Acosta**[b], **Gefei Chen**[b], **Michael Landreh**[c], **Alexey Lyashkov**[d], **Miguel A. Aon**[d], **Luigi Ferrucci**[d], **Ruth Shimmo**[a], **Jan Johansson**[b], **Ruin Moaddel**[d,*]

[a]School of Natural Sciences and Health, Tallinn University, Tallinn, Estonia

[b]Department of Biosciences and Nutrition, Karolinska Institutet, 14183, Huddinge, Sweden

[c]Department of Microbiology, Tumor and Cell Biology, Karolinska Institutet, Solna, Sweden

[d]Biomedical Research Centre, National Institute on Aging, NIH, Baltimore, MD, 21224, United States

Abstract

Human integral membrane protein 2B (ITM2B or Bri2) is a member of the BRICHOS family, proteins that efficiently prevent Aβ42 aggregation via a unique mechanism. The identification of novel Bri2 BRICHOS client proteins could help elucidate signaling pathways and determine novel targets to prevent or cure amyloid diseases. To identify Bri2 BRICHOS interacting partners, we carried out a 'protein fishing' experiment using recombinant human (rh) Bri2 BRICHOS-coated magnetic particles, which exhibit essentially identical ability to inhibit Aβ42 fibril formation as free rh Bri2 BRICHOS, in combination with proteomic analysis on homogenates of SH-SY5Y cells. We identified 70 proteins that had more significant interactions with rh Bri2 BRICHOS relative to the corresponding control particles. Three previously identified Bri2 BRICHOS interacting proteins were also identified in our 'fishing' experiments. The binding affinity of Glyceraldehyde 3-phosphate dehydrogenase (GAPDH), the top 'hit', was calculated and was identified as a strong interacting partner. Enrichment analysis of the retained proteins identified three biological pathways: Rho GTPase, heat stress response and pyruvate, cysteine and methionine metabolism.

*Corresponding author at: 8C220 BRC, 251 Bayview Blvd., Baltimore, MD, United States. moaddelru@mail.nih.gov (R. Moaddel).

Author contributions

RM, JJ and RS directed and supervised the project and design of the work. HT, NK, AA, LGA, GC, AL, MAA and ML performed experiments, analyzed data and commented on the paper. HT, NK, AA, LF, RS, JJ and RM contributed to the interpretation of the data. HT, JJ and RM prepared the manuscript. All authors have contributed to and approved the final version of the manuscript.

Appendix A. Supplementary data

Supplementary material related to this article can be found, in the online version, at doi:https://doi.org/10.1016/j.jpba.2021.113996.

Declaration of Competing Interest

The authors declare that they have no known competing financial interests or personal relationships that could have appeared to influence the work reported in this paper.

Keywords

Human integral membrane protein 2B (ITM2B or Bri2); Protein Fishing; Untargeted proteomics; Glyceraldehyde 3-phosphate dehydrogenase (GAPDH) was identified as a strong interacting partner

1. Introduction

Proteins are marginally stable in their native structures and hydrophobic parts that are exposed upon partial unfolding have a tendency to form intermolecular contacts that lead to protein aggregation [1]. Misfolding and aggregation are thus inherent to the life of proteins and nature has developed molecular chaperone systems that are specialized in preventing aggregation of client proteins, but there is evidence that these mechanisms become dysfunctional in aging [2]. Interestingly, a screen in aging *Caenorhabditis elegans* nematodes found that expression of small heat shock proteins (Hsp) strongly correlated with longevity, possibly through the sequestration of protein aggregates [3]. Different molecular chaperone families work by different mechanisms; for example, the cage chaperones like GroEL enclose their clients and allow them to fold without the risk of encountering other unfolded proteins, while the Hsp 70 and 90 families bind and release client proteins in cyclic and energy (ATP) dependent manners. The small Hsp family members work by a simpler, ATP independent mechanism, which relies on binding to exposed nonpolar client regions [4]. Molecular chaperones are mainly found intracellularly, but extracellular chaperones have also been described, for example the lipoprotein associated protein clusterin (apolipoprotein J) can prevent aggregation of several clients and was recently found to be able to bind extracellular misfolded proteins, including the Alzheimer's disease (AD) associated amyloid-peptide (Aβ), and transfer them into cells for degradation [5]. Amyloid formation is a special case of protein misfolding that is associated with about 40 human diseases, including some of the most common and morbidity-associated diseases like AD, Parkinson disease, and type 2 diabetes [6]. Amyloid is highly regular and structured, which contrasts qualitatively to traditional amorphous protein aggregates that are non-fibrillar [2]. In AD, the Aβ forms amyloid that eventually ends up in extracellular plaques, but the most neurotoxic derived species is probably rather oligomeric assemblies that can diffuse and cause neuronal dysfunction and eventual death by largely unknown mechanisms [7]. We have found that an endogenous defense (the BRICHOS domain) against amyloid fibril formation and toxicity holds the potential to be translated to treatment for aggregation, neurotoxicity and neuroinflammatory effects of Aβ in AD [8]. The BRICHOS domain counteracts amyloid aggregation differently than any of the therapeutic approaches attempted so far [8]. Thus, surfactant protein C (SP-C) is an amyloid-forming protein, and proSP-C contains a BRICHOS domain that prevents β-sheet aggregation during biosynthesis, thereby promoting formation of the native α-helical SP-C conformation [9]. Mutations in proSP-C BRICHOS domain result in amyloid formation of the SP-C part and lethal amyloid lung disease in early childhood [9]. Since most known diseases characterized by amyloid deposition occur late in life, these observations strongly support the hypothesis that BRICHOS is fundamental for the prevention of amyloid diseases and that interference with BRICHOS could be effective in amyloid disease prevention. Indeed, it has been found

that the BRICHOS domain can prevent amyloid formation not only of its physiological clients but also of other amyloidogenic proteins, including Aβ and islet amyloid polypeptide (IAPP) associated with type 2 diabetes [10].

Further studies of BRICHOS domains, in particular from Bri2 (mutations of which cause familial British or Danish dementias with amyloid in the Central Nervous System (CNS) [11]) have revealed that BRICHOS efficiently prevents Aβ42 aggregation via a unique mechanism and, importantly, reduces Aβ42 neurotoxicity to mouse hippocampal slice preparations [12–15]. BRICHOS prevention of Aβ42 toxicity to hippocampal slices can be translated to animal models; transgenic expression of BRICHOS domains in *Drosophila* flies that overexpress Aβ42 results in reduced Aβ aggregation as well as improved life-span and mobility [15]. Recombinant human (rh) Bri2 BRICHOS forms different assembly states, of which the monomer is the most efficient in preventing Aβ42 neurotoxicity, while oligomers composed of 20–30 subunits are very efficient in preventing non-fibrillar aggregation of destabilized model proteins [12]. From these observations, it is clear that rhBri2 BRICHOS is able to bind to several different proteins. However, a majority of these proteins probably remain unknown. Currently, co-immunoprecipitation remains the primary method used to identify client proteins. A recent study identified a Bri2 interactome, where three brain regions were processed by Bri2 immunoprecipitation and co-precipitating proteins were identified by Nano-HPLC-MS/MS [16]. In that study, the proteins found were associated with neurite outgrowth, neuronal differentiation and synaptic signaling and plasticity but it is unknown whether the BRICHOS domain, which represents about 100 residues of the 266 amino acids full length Bri2 protein, is involved in the interactions found. A limitation of this approach is that it requires the use of a selective antibody and as a result, it can isolate additional proteins based on the selectivity of the antibody.

The identification of novel Bri2 BRICHOS client proteins could help elucidate signaling pathways and determine novel targets for combatting amyloid diseases. Recently, ligand fishing, a process by which a protein is immobilized onto a magnetic particle to ‘fish out’ active components from a complex matrix has been extensively used to identify novel ligands from natural products [17,18]. It was also demonstrated that the protein coated magnetic particles can form protein complexes with recombinant proteins. [19]. Specifically, Hsp90-α was immobilized onto the surface of magnetic beads and formed a protein complex with Hsp70 only in the presence of the HSP70-HSP90 Organizing Protein (HOP) [19]. In that study, the HSP90-α coated magnetic beads were able to retain p60-HOP from KU-812 basophile lysates, in a targeted fishing experiment using western blot analysis [19]. Combining the ‘protein fishing’ experiments with untargeted proteomic analysis could help identify novel binding proteins for the immobilized target. To this end, herein we describe a novel ‘protein fishing’ experiment that would help elucidate proteins that interact with Bri2 BRICHOS using an unbiased proteomics approach.

2. Materials and methods

2.1. Materials

Experiments were conducted with recombinant human (rh) Bri2 BRICHOS gene sequence coding for the human Bri2 BRICHOS domain (90–236), corresponding to amino acid

(NP 068839.1) ligated into the pET-32c(+) vector (Novagen) (Protein Fishing). For surface plasmon resonance (SPR), gene fragments encoding rh Bri2 BRICHOS domain (113–231) (~14.1 kDa) and an efficient solubility tag derived from the N-terminal domain of spider silk proteins (NT*) were cloned into a modified pET vector [20]. The Bri2 BRICHOS (90–236) domain was expressed as a fusion protein with N-terminal Thioredoxin tag (Trx), 6 × Histidine tag (His), and Solubility-tag (S-tag) in *Escherichia coli* (*E. coli*) SHuffle T7 Express cells (New England Biolabs Inc. Ipswich, MA). Trx-His was cleaved off by thrombin (from bovine plasma, 50 NIH-U/mg. Merck, Burlington, MA), leaving the rh Bri2 BRICHOS domain (90–236) (~20.4 kDa) [21]. The rh Bri2 BRICHOS domain (113–231) was expressed as a fusion protein with N-terminal His6, NT*-tag and thrombin cleavage site in *E. coli* SHuffle T7 Express cells [12]. His6-NT* was cleaved off by thrombin, leaving the rh Bri2 BRICHOS domain (113–231) (~14.1 kDa). Gene sequence coding for the human Aβ 1–42 peptide together with start codon ATG was ligated into PetSac plasmid vector (modified from Pet3a with *Nde*I and *Sac*I cloning sites) [22]. Recombinant human Aβ 1–42 peptide was expressed with an N-terminal methionine ($_{rh}$Aβ1–42, ~4.7 kDa) in *E. coli* BL21 (DE3) pLysS Star cells (Invitrogen, Thermo Fisher Scientific, Waltham, MA). Apolipoprotein A-I (Apo-AI, purified from human plasma with >98 % purity) was purchased from Chemicon, Sigma-Aldrich (St. Louis, MO). Recombinant human glyceraldehyde 3-phospate dehydrogenase (GAPDH with >95 % purity) purchased from Thermo Fisher Scientific (Waltham, MA).

Acetonitrile, ammonium bicarbonate, benzamidine, chloroform, dithiothreitol (DTT), 1-Ethyl-3-(3-dimethylaminopropyl)carbodiimide hydrochloride (EDC), glutaraldehyde, hydroxylamine, imidazole, iodoacetamide, 2-(N-morpholino)ethanesulfonic acid hydrate (MES), methanol, N-hydroxysulfosuccinimide (Sulfo-NHS, 98+%), phenylmethyl-sulfonyl fluoride (PMSF), pyridine, sodium azide (NaN_3), sodium cyanoborohydride ($NaBH_3CN$, 95 %), Thioflavin T (ThT), thiourea, trifluoroacetic acid (TFA), Tween 20 and urea were purchased from Sigma-Aldrich (St. Louis, MO). BCA protein assay kit from Pierce (Thermofisher Scientific, Waltham, MA), Bradford reagent, formic acid, sodium phosphate buffer [20 mM, pH 8.0] (PB), phosphate-buffered saline [20 mM, pH 7.4] containing 0.15 M NaCl (PBS) and 1xPBS were purchased from Thermo Fisher Scientific (Waltham, MA). Trypsin/lysC mixture was purchased from Promega (Madison, WI). Protease inhibitor cocktail was purchased from Merck (Burlington, MA). DEAE-cellulose was purchased from Santa Cruz Biotechnology Inc. (Dallas, TX). IMAC media (Ni Sepharose™ 6 Fast Flow) was purchased from GE Healthcare (Chicago, IL). BcMag amine-terminated magnetic beads (50 mg/mL, 1 μm) were purchased from Bioclon Inc (San Diego, CA). Deionized water was obtained from a Milli-Q system (Millipore, Billerica, MA).

2.2. Immobilization of rhBri2 BRICHOS domain onto MB

2.2.1. Bri2-NT-MB—rhBri2 BRICHOS domain was immobilized via a previously published method, with slight modifications [17–19]. Briefly, 25 mg of BcMag magnetic beads (MB) were placed in a 2 mL microcentrifuge tube. The MBs were washed three times with 1 mL of coupling buffer (pyridine [10 mM, pH 6.0]) and were suspended in 1 mL of 5 % glutaraldehyde solution in coupling buffer and rotated for 3 h at room temperature (RT). After separation using the manual magnetic separator (Dynal MPC-S,

Invitrogen Corporation, Carlsbad, CA), the MBs were washed three times with 1 mL of coupling buffer. A suspension of 200 μg of (rh) Bri2 BRICHOS (90–236) domain in 500 μL of coupling buffer containing 1 % sodium cyanoborohydride was added to the activated MBs. The reaction was left for 7 days at 4 °C with gentle rotation. The supernatant was discarded and 200 μL of coupling buffer containing 100 mM hydroxylamine and 2.5 % cyanoborohydride was added. The mixture was shaken overnight at RT with gentle rotation. The supernatant was discarded and MBs were washed 3x with 1 mL of 1xPBS (containing 0.02 % NaN_3). The control hydroxylamine-coated (NT)-MB (Control-MB) were made in the same manner but without the addition of rhBri2.

2.2.2. Bri2-CT-MB—Rh Bri2 BRICHOS domain was immobilized via carboxylic acid amino acid residues following a previously published method, with slight modifications [18,19]. Briefly, 25 mg of MBs was rinsed with 1 mL of MES [100 mM, pH 5.5] in a 2 mL microcentrifuge tube. After magnetic separation, the supernatant was discarded, and the MBs were suspended in 300 μl of MES [100 mM, pH 5.5] and 200 μg of rhBri2. 50 μl of a mixture of 10 mg of EDC and 15 mg of sulfo-NHS in 1 mL of deionized water were added and the mixture was vortex-mixed for 5 min and left for 3 h at 4 °C with gentle rotation. This was followed by the addition of 20 μl of 1 M hydroxylamine, and the mixture was left for 30 min at 4 °C with gentle rotation. The supernatant was discarded, and the MB was rinsed three times with 1 mL of 1xPBS containing 0.02 % NaN_3.

2.3. Analysis of the MB activity by Aβ 1–42 aggregation kinetics

Bri2-MBs and reduced Bri2-MBs were mixed with 3 μM rh Aβ 1–42 in PB containing 10 μM ThT and pipetted onto a 96-well plate (Corning Inc, Corning, NY). The ThT fluorescence was recorded using a FLUOstar OPTIMA plate reader (BMG Labtech, Germany), as described above. Samples were repeated in quadruplicate. Reduction of rhBri2-NT-MB, rhBri2-CT-MB and Control-MB were carried out with 1 mM DTT for 1 h at RT, after which the supernatant was removed using the Dynal Magnetic separator (reduced Bri2-MBs). Aggregation kinetics was monitored at RT with shaking (shaking 60 s before each measuring cycle, 200 rpm, 250 cycles, cycle time 300 s, 10 flashes per well and cycle, 0.2 s positioning delay, orbital averaging 2 mm, gain set to 2000) for up to 6 h, using upper optics with 440 nm excitation filter and 480 nm emission filter. Data was sent to OTIMA Data Analysis software, where the average of the replicates was transported to Microsoft Excel software for normalization. The time evolution of fibril formation of 3 μM Aβ42 with Control-MB, Bri2-NT-MB and Bri2-CT-MB were fitted to a sigmoidal equation using OriginPro 2020b software (OriginLab, Northampton, MA) from which aggregation half-time $t_{1/2}$ was extracted. The MBs were removed from the 96-well microplate and the supernatant was discarded.

2.4. SH-SY5Y cells

Human SH-SY5Y cells were cultured in Dulbecco's Modified Eagle's Medium and Ham's F12 culture medium (DMEM-F12 with GlutaMAX) (Thermo Fisher Scientific, UK) supplemented with 10 % (v/v) fetal bovine serum (FBS) (Thermo Fisher Scientific, UK) at 37 °C in a humidified atmosphere with 5 % (v/v) CO_2. Cells were maintained in T-175 sterile plastic culture flasks. The adherent cells were continuously cultivated and grown

nearly to 80–90 % optical confluence, before they were detached by Gibco™ TrypLE™ solution (ThermoFisher Scientific, UK), and collected by adding fresh pre-warmed growth medium to the culture flask.

2.5. Protein fishing experiments

SH-SY5Y cells (ATCC, Mannassas, VA) were collected (2.5×10^6 cells) and suspended in 2 mL of homogenization buffer (Tris-HCl [50 mM, pH 8.0] containing 5 mM EDTA, 1 mM benzamidine, 0.1 mM PMSF plus 10 μL protease inhibitor cocktail (Roche)) and homogenized with a Kontes Pellet Pestle (Sigma-Aldrich, St.Louis,MO). The mixture was centrifuged at 100,000 × g for 30 min at 4 °C and the cytosolic fraction (supernatant) was collected for protein fishing experiment. The cytosolic fraction (1 mL) was added to the Bri2-NT-MBs (3 replicates) and Control-MBs (3 replicates) and mixed at 15 rpm at RT for 30 min. The supernatant (Load) was removed by using the Dynal magnetic separator (3 min). The Bri2-NT-MBs were washed twice with 1 mL of 1x PBS for 2 min. Each wash was collected after separation using the Dynal magnetic separator (2 min) (Wash 1, 2, respectively). Bound proteins were then eluted by incubating with a saturating concentration of rh Bri2 BRICHOS (10 μM, 1 mL) for 30 min at RT (Elute 1) followed by a wash (Elute 2). After, the elutes were collected, the Bri2-MB were washed once with 1xPBS (Wash 3). All the collected supernatants (load, elute 1, elute 2) were lyophilized and kept at −80 °C until digestion. All samples were run in triplicate, with the exception of the Loading buffer for the Bri2-NT-MBs, which had five replicates and the Control-MB Elution 1, which had 3 replicates, however, one was lost during the proteomic analysis.

2.6. Proteomic analysis

Protein concentration in the supernatants was determined by BCA protein assay, following manufacturers protocol. The lyophilized samples were dissolved in 30 μl 1x PBS and mixed with 270 μl of methanol:chloroform:water (5:1:3 ratio), vortexed and centrifuged at 15000 ×*g* for 2 min. The supernatant was discarded, and the pellet was mixed with 500 μl methanol, vortexed and centrifuged at 15 000 ×g for 2 min at 4 °C. The was repeated twice. Digestion was carried out as previously described [23]. Briefly, the resulting pellet was resuspending in 30 μl of a solution of 8 M urea, 2 M thiourea, 150 mM NaCl, 100 mM DTT, pipetted for 5 min and vortexed and incubated with shaking (500 rpm) for 1 h at 37 °C. Iodoacetamide was added to a final concentration of 150 mM and incubated for 1 h at 37 °C in the dark. The samples were diluted to 360 μl with 50 mM ammonium bicarbonate, then trypsin/lysC mixture was added to a final 10 ng/μl concentration and the sample was incubated at 37 °C overnight with shaking at 1000 rpm. 36 μl of formic acid was added and the solution was dried using a SpeedVac Concentrator (Savant SPD111V SpeedVac Concentrator, Thermo Scientific, Waltham, MA).

Protein digests were desalted as previously described [23]. Briefly, protein digests were resuspended in 100 μl of deionized water containing 5 % acetonitrile and 2 % TFA. Samples were desalted on a Resteck-C18 guard cartridge (10 × 4.0 mm) using Agilent 1260 Bio-inert HPLC system connected to the fraction collector with UV detector at 214 nm. The separation was achieved at a flowrate of 0.450 mL/min at 35 °C with a 15 min run time. Mobile Phase A (water with 0.1 % TFA) and Mobile Phase B (90 % acetonitrile with

0.1 % TFA) were used with the following gradient: 0 min 5 %B; 6 min 5 % B, 6.1 min 95 % B; 10 min 95 % B; 10.1 min 5 % B. The peptide peak was collected between 7.2–9.0 min. Autosampler and fraction collector were kept at 4 °C. The desalted samples were then dried by SpeedVac and stored at −80 °C until analysis.

The samples were dissolved in 5 μl of water containing 5 % acetonitrile and 0.1 % formic acid. Purified peptides were analyzed as previously described [23]. Briefly, they were analyzed using UltiMate 3000 Nano LC Systems coupled to the Orbitrap Fusion Lumos Mass Spectrometer (Thermo Scientific, San Jose, CA) with the heated capillary temperature +320 °C and spray voltage set to 2.5 kV. Each sample was separated on a 45 cm capillary column (Ultra C18 silica, 5 μm) with 150 μm ID on a linear organic gradient using 550 nl/min flow rate. Gradient went from 5 to 35 %B in 80 min. Mobile phases A and B consisted of 0.1 % formic acid in water and 0.1 % formic acid in acetonitrile, respectively. Full MS1 spectra were acquired from 330 to 1600 m/z at 60000 resolution and 40 ms maximum accumulation time with automatic gain control [AGC] set to 1×10^6. MS/MS spectra were resolved to 15 000 with 100 ms of maximum accumulation time and AGC target set to 1×10^5. Fifteen most abundant ions were selected for fragmentation using 36 % normalized high collision energy. A dynamic exclusion time of 70 s was used to discriminate against the previously analyzed ions. RAW data files were converted to mgf data format using software MSConvert. The chosen parameters for the conversion were: Binary encoding precision 32-bit; TPP compatibility; Activation HCD; Threshold count 900 most-intense; zeroSamples remove Extra 1-; peakPicking true 1-. Mgf data files were next transferred to MASCOT protein identification software. The chosen parameters for the protein identification were: Database Sprot human; Decoy database; Monoisotopic mass; Enzyme Trypsin/P; Max missed cleavages 2; Variable modifications - carbamidomethyl (C), carbamyl (K), carbamyl (N-term), oxidation (M), deamidated (NQ); peptide charge state: 2+ and 3+; Report top AUTO; Peptide tol: 20 ppm; #C13 – 0; no determined protein mass; MS/MS ions search; Data format mascotgeneric; MS/MS tol. ± 0.08 Da; No quantitation; Instrument ESI-TRAP and no error tolerant search. MASCOT Data file exports search result automatically to biospec.nih.gov page, from where the file was saved. Further, the file was loaded and analyzed by Scaffold Q + software. For loading and sample analysis the following parameters were chosen: spectrum counting; database Sprot human 02062017; Analyze with X! Tandem; Peptide prophet scoring; Protein cluster analysis; no annotation; generate decoy proteins. Final results were transferred to Microsoft Excel software.

2.7. Surface plasmon resonance

SPR assays were performed in a BIAcore 3000 instrument (BIA-core AB, Uppsala, Sweden). Rh Bri2 BRICHOS (113–231) (30 μg/mL) was diluted in sodium acetate [10 mM, pH 4.5], and was individually immobilized by amine coupling onto flow cells (Fc) on CM5 sensor chips (GE Healthcare, Chicago, IL) to reach immobilization levels of around 5800 RU. Blank reference surfaces were prepared on each sensor chip using the same coupling protocol only with no protein injected. All immobilization experiments were performed with HEPES [10 mM, pH 7.4] containing 150 mM NaCl, 0.2 mM EDTA as running buffer, a flow rate of 20 μL/min and otherwise according to the manufacturer's instructions for the amine coupling kit (GE Healthcare, Chicago, IL). After immobilization the flow-cells were

stabilized over-night in running buffer at a flow rate of 20 μL/min to remove unspecifically bound protein.

Lyophilized Apo-A1 and GAPDH were dissolved to 1 mg/mL each in running buffer. Apo-A1 was diluted to 5 different monomer concentrations between 1.1 μM – 17.7 μM. GAPDH was diluted to 7 different tetramer concentrations between 0.039 μM – 2.5 μM. The samples were individually injected over the chip surfaces containing immobilized rh Bri2 BRICHOS (Fc 2) and blank (Fc 1) at 25 °C and at a flow rate of 20 $\mu L/min^{-1}$ (Apo-A1) or 30 $\mu L/min^{-1}$ (GAPDH). The chip surfaces were regenerated between each sample of analyte by injection of 10 mM NaOH for 30 s for Apo-A1 or 0.1 % SDS for 2 × 30 s for GAPDH at a flow rate of 30 $\mu L/min^{-1}$. Double referencing was performed by subtracting the response from the blank surface and the response from a blank injection (zero analyte concentration) from the immobilized surface response for each concentration of analyte. Steady state affinity for Apo-A1 or GAPDH to immobilised rh Bri2 BRICHOS was estimated by plotting the maximum binding response versus concentration. The data was fitted by nonlinear regression using a 1:1 binding model.

2.8. Native mass spectrometry of Apo-A1 and GAPDH

Immediately prior to MS analysis, proteins were buffer-exchanged into ammonium acetate [100 mM, pH 7.0], using Bio-Spin 6 microspin filters (Bio-Rad). Mass spectra were acquired on a Micromass LCT ToF modified for analysis of intact protein complexes (MS Vision, The Netherlands) equipped with an offline nanospray source. Samples were injected directly using gold-plated borosilicatecapillaries (ThermoScientific). The capillary voltage was 1.5 kV and the RF lens 1.5 kV. The cone voltage was 100 V and the pressure in the ion source was maintained at 9.0 mbar. Spectra were analyzed using the MassLynx 4.1 software package (Waters, UK).

2.9. NMR

Nuclear magnetic resonance (NMR) experiments were performed at 37 °C on a 700 MHz Bruker spectrometer using a 3 mm shigemi NMR tube. BEST-TROSY pulse sequences were applied using 1194 × 256 complex points. A stock solution of 32 μM Apo-A1 was titrated onto 180 μM ^{13}C-^{15}N Bri2 BRICHOS R221E monomer [13] in 20 mM sodium-phosphate buffer, pH 7.2, 0.2 mM EDTA, 0.02 % NaN_3, 10 % D_2O, where the sample volume was hold constant to 170 μL throughout the whole titration series. The final concentration for both proteins was 27 μM at final 1:1 molecular ratio. Due to the sample dilution different number of scans were used during the titration experiment. Spectra were processed in Topspin 4.0 and visualized in Sparky.

2.10. Enrichment analysis

Clustering of proteins was performed with STRING protein–protein interaction database (https://version-11-0.string-db.org/cgi/network). STRING analysis was used on the proteins identified in each fraction (load, elute 1, elute 2). Interacting proteins were not included in the analysis. A “protein social network” was constructed for each fraction and combined. The inclusion of the 266-residue full-length Bri2 protein (ITM2B), whereof the BRICHOS domain constitutes approximately residues 120 to 231 [24], to the protein social network

was also done for each fraction as an internal standard to determine its impact on the degree of confidence.

3. Results and discussion

To identify rh Bri2 BRICHOS client proteins, we developed a ‘protein fishing’ method where the target protein is immobilized onto the surface of a magnetic bead and incubated with cell homogenates and the retained proteins are collected and characterized by proteomic analysis. To this end, rh Bri2 BRICHOS protein was immobilized onto the surface of magnetic beads (MB) via the N-terminal amino group (Bri2-NT-MB) or a carboxylic acid group (Bri2-CT-MB).

3.1. Characterization of Bri2-NT-MB and Bri2-CT-MB

Kinetics analysis of 3μM Aβ42 fibril formation was carried out in the presence of rhBri2 BRICHOS domain, either bound to MBs or free in solution, using the ThT fluorescence assay. Aβ42 plus the control-MB in the absence of rhBri2 BRICHOS, resulted in a typical sigmoidal response curve with aggregation of half time ($t_{1/2}$) of 1.0 h and rapid fibril formation plateauing within 2 h (Fig. 1). In the presence of control-MB plus free rhBri2 BRICHOS (positive control), a significant delay in fibril formation was observed ($t_{1/2}$ = 3.6 h). Bri2-NT-MBs incubation with 3μM Aβ42 resulted in a significant delay ($t_{1/2}$ = 3.8 h) of fibril formation (Fig. 1), while the Bri2-CT-MB resulted in only a slight delay in the fibril formation ($t_{1/2}$ = 1.2 h). As a result of the retained activity of the rhBri2 BRICHOS only on the Bri2-NT-MBs, these beads were used for the ‘protein fishing’ experiments. rhBri2 BRICHOS has been demonstrated to exist as monomers, dimers and oligomers [12], with monomers and dimers more effectively suppressing Aβ42 fibril formation with the ThT fluorescence assay [12]. The intra- and intermolecular disulfides of the Bri2 BRICHOS domain can be reduced to free thiols in the presence of DTT. The addition of DTT resulted in a subtle increase in activity with the Bri2-NT-MBs ($t_{1/2}$ = 4.44 h) (Fig. 1). The reduction of the Bri2-NT-MBs resulted in a loss of ~20 % of immobilized protein, suggesting that rhBri2 BRICHOS was predominantly immobilized in the intramolecular disulfide linked monomeric form. This is consistent with the observation, that the Bri2-NT-MBs inhibited Aβ42-fibril formation to a greater extent than the positive control, a mixture of rhBri2 BRICHOS oligomers, dimers and monomers. While the Bri2-NT-MB were successfully used for the ThT fluorescence assay, they were limited to single use experiments, as formic acid (70 %) was required to remove fibrils, which resulted in a decrease of activity of the immobilized rhBri2 (data not shown).

3.2. Protein fishing

Protein fishing experiments were carried out on the human neuroblastoma cell line, SH-SY5Y, as it was previously demonstrated that recombinant $BRI2_{76–266}$ induced the activation of the apoptosis pathway in this cell line [25]. SH-SY5Y cells were homogenized and centrifuged generating the cytosolic fraction (supernatant), which was incubated with the Bri2-NT-MBs and the corresponding Control-MBs. The removal of the MBs resulted in the Load fraction and after two washes, a saturating concentration of rh Bri2 BRICHOS was used to generate the Elute 1 fraction and a subsequent wash resulted in Elute 2

fraction (Table 1 and Supplemental Table 1) (Scheme 1). Protein hits were identified by two approaches: 1) a significant difference in spectral counts between the Bri2-NT-MB and corresponding control in the Elute fractions, and 2) The absence or decreased presence of a protein, based on spectral counts, in the Load fraction with a concurrent increase in the Elute fractions relative to control.

Using the first approach, 70 proteins were identified that had a significant increase ($p < 0.05$) in elution from the Bri2-NT-MB relative to Control-MB, with GAPDH having the largest spectral difference ($\Delta = 576$) and RANBP1 being the most significant ($\Delta = 9.67$) (Table 1 and Supplemental Table 1). Several of these proteins have been previously identified as interacting partners for Bri2, including Neuronal cell adhesion molecule (NRCAM) and Neuromodulin [24]. In addition to GAPDH, several other proteins had large spectral differences between Bri2-NT-MB and Control-MB, including CKB, PTMA, PTMS, GDI2, GDI1 with a $\Delta \approx 50$ and HSPA4, ARHGDIA, ANXA6, NRCAM, with a $\Delta \approx 25$ (Table 1 and Supplemental Table 1). Citrate synthase (CS) was also identified, which is consistent with recent studies demonstrating that rh Bri2 and Bri3 BRICHOS domains bind and efficiently inhibit non-fibrillar aggregation of thermo-denatured CS [12,18]. In the second approach, only Apo-A1 and C3 were present in smaller amounts in the Bri2-NT-MB Load Fraction, with concurrent increases in the Bri2-NT-MB Elute 1 and Elute 2 fractions, although the difference was not significant in any fraction. The data from the ‘protein fishing’ experiments, clearly point out that future ‘protein fishing’ experiments should be conducted using the first approach, as it resulted in the identification of 70 significant hits.

3.3. Study of direct interaction with rhBri2 BRICHOS

In order to study direct interactions, rh Bri2 BRICHOS was immobilized onto sensor chip surfaces via amines and interactions with GAPDH and Apo-A1 were studied by Surface Plasmon Resonance (SPR). GAPDH was shown to interact with rh Bri2 BRICHOS by SPR with an apparent binding affinity of K_D of 2.76 μM (Fig. 2A). Native mass spectrometry (Supplemental Fig. 1) revealed that GAPDH forms tetramers and as a result, the apparent binding affinity (K_D) of GAPDH for the immobilized rhBri2 BRICHOS was calculated based on tetramer concentrations to be K_D of 0.69 μM ($r^2 = 0.996$). This identifies for the first time that GAPDH is a strong interacting partner with rh Bri2 BRICHOS. Interactions between Apo-A1 and rh Bri2 monomers was also studied by SPR. Apo-A1 had an apparent binding affinity K_D of 6.7 μM ($r^2 = 0.960$) with an R_{max} of 21.81 response units (RU) calculated based on monomer concentrations, determined by Native MS (Suppl Fig. 1). This is a lower boundary estimate as the plateau binding was not reached at the highest concentration of 17.65 μM. The maximal signal intensity/R_{max} for GAPDH was 690 RU, significantly higher than what was observed with Apo-A1. As GAPDH and Apo-A1 have comparable molecular weights, this supports the finding by Native MS that Apo-A1 is monomeric, whereas GAPDH is in a tetrameric form, consistent with previous studies [26]. As a result of the weak interactions observed by SPR for Apo-A1, NMR experiments were carried out in order to determine whether any interactions are present between rh Bri2 BRICHOS and Apo-A1. However, the wild type rh Bri2 BRICHOS did not result in satisfactory spectra (data not shown), as a result, 180 μM ^{13}C-^{15}N Bri2 BRICHOS R221E monomer was used [13]. The NMR spectrum demonstrated that no interaction or only

weak interaction was observed between Apo-A1 and rh Bri2 BRICHOS in solution at 1:1 molecular equivalents (Suppl. Fig. 2), as no chemical shift changes were observed. While inconsistent with the SPR experiments, the differences observed may result from the fact that NMR was carried out at 37 °C and/or that the mutant rh Bri2 BRICHOS R221E had to be used instead of the wild type rhBri2 BRICHOS (113–231) domain used in the SPR or the rh Bri2 BRICHOS (90–236) domain utilized in the MB protein fishing experiments. It has recently been shown that wt rh proSP-C BRICHOS and mutant thereof, rh prosP-C BRICHOS T187R that is analogous to rh Bri2 BRICHOS R221E bind with different affinities to Aβ fibrils [27]. The NMR results cannot rule out that there is a dynamic exchange between free, as the major state, and bound rh Bri2 BRICHOS, as the minor state, however, the NMR signal intensities could not be compared due to the large dilution effect that made different number of scans for each experiment necessary. Such a mechanism would be characterized by a weak binding constant, which would be in agreement with the SPR data, as well as the ‘fishing’ data, where a lack of significance was observed in the Load, Elute 1 and 2 fractions. The identification of a strong interacting partner, GAPDH, and a weak interacting partner, ApoA1, in the ‘protein fishing’ experiment, demonstrates that saturation of Bri2-NT-MB was not obtained in the ‘fishing’ experiments.

3.4. Enrichment analysis

In order to help provide insight into a potential mechanism of action of rh Bri2 BRICHOS, STRING analysis was performed with proteins that were significantly different in the Elute 2 fraction to construct a “protein social network”. Three protein clusters, Rho GTPase, heat stress response and pyruvate, cysteine and methionine metabolism were identified (Fig. 3). The inclusion of full-length Bri2 (also known as integral membrane protein 2B, ITM2B) to the protein social network did not result in any change with the list of proteins, indicating that Bri2 is not known to be involved with any of the identified clusters. Interestingly, while Bri2 did not result in any change to the protein social network, a recent study suggested that proteins associated with the Bri2 protein were involved in neurite outgrowth, neuronal differentiation and synaptic signaling and plasticity [16]; the identified clusters in this study are known to be involved in these signaling pathways [28–30]. These results may help provide additional insight into the mechanism of Bri2 BRICHOS domain from a molecular perspective. However, these results should be interpreted with care, as these findings need to be validated with additional experimental evidence.

In our study, four proteins from the Rho GTPase cluster were identified, including ARHGDIA, ARHGDIB, GDI1 and GDI2. Rho GTPases have been shown to be dysregulated in AD and to play a critical role in neurological disorders and AD pathogenesis [31] and are considered a potential therapeutic target in AD. ARHGDIA has been shown to play a role in the maintenance of the neuronal cytoskeleton, promotion of neuronal development, neurite outgrowth [32] and to possess antiapoptotic activity. Rho GTPase regulatory proteins have also been shown to control synapse development and plasticity [28]. Inclusion of the proteins from the load fractions resulted in a connection between the Rho GTPase and the second cluster of the heat stress response via proteins from the fibrin clot including Apo-A1 (data not shown). The second cluster identified was the heat stress response cluster. Several of the heat shock proteins were identified with a high

degree of confidence, including HSPA8, HSPA4 (HSP 70 family) and HSPA2. Small Heat Shock Proteins (sHsps) have been found to co-localize with amyloid plaques associated with AD and other neurodegenerative diseases [33], suggesting that the cellular quality control machinery is activated to prevent accumulation of misfolded species. Hsps may be involved in neurodevelopment through pathways that regulate cell differentiation, neurite outgrowth and cell migration [29] and involved in homeostatic synaptic plasticity [30], consistent with a recent study on the signaling pathways identified with proteins associated with Bri2 [16]. Bri2 and Bri3 have also been found in close proximity to Aβ plaques in AD patients [34]. The Heat Stress response cluster is connected to the third cluster (the pyruvate, cysteine and methionine metabolism cluster) via GAPDH, the protein that had the largest spectral difference between the Bri2-NT-MB and the Control-MB. GAPDH, a key enzyme in glycolysis, also plays a role in DNA repair, transcriptional regulation, membrane fusion and transport, autophagy and cell death [35]. GAPDH aggregates have been shown to accelerate Aβ amyloidogenesis and subsequent neuronal cell death both *in vitro* and *in vivo* and have been found post-mortem in the brains of patients with AD [35].

The proteomic data and enrichment analysis obtained in the fishing study, confirm that the novel application of ‘protein fishing’ is a viable approach that in combination with proteomics offers a significant advantage in the identification of new interacting partners thus providing insight into novel mechanisms. The approach was able to identify interacting partners with an order of magnitude differences in the binding affinities.

Supplementary Material

Refer to Web version on PubMed Central for supplementary material.

Acknowledgements

This research was supported by the Intramural Research Program of the National Institute on Aging, NIH. This research has been supported by the Tallinn University Research Fund project TF1515 (HT, RS) and the Tallinn University ASTRA project “TU TEE - Tallinn University as a promoter of intelligent lifestyle” financed by the European Union European Regional Development Fund 2014-2020.4.01.16-0033 (HT, RS).

References

[1]. Dobson CM, Protein misfolding, evolution and disease, Trends Biochem. Sci 24 (1999) 329–332. [PubMed: 10470028]

[2]. Hipp MS, Kasturi P, Hartl FU, The proteostasis network and its decline in ageing, Nat. Rev. Mol. Cell Biol 20 (2019) 421–435. [PubMed: 30733602]

[3]. Walther DM, Kasturi P, Zheng M, Pinkert S, Vecchi G, Ciryam P, Morimoto RI, Dobson CM, Vendruscolo M, Mann M, Hartl FU, Widespread proteome remodeling and aggregation in aging C. elegans, Cell 161 (2015) 919–932. [PubMed: 25957690]

[4]. Carra S, Alberti S, Arrigo PA, Besesch JL, Benjamin IJ, Boelens W, Bartelt-Kirbach B, Brundel BJJM, Buchner J, Bukau B, Carver JA, Ecroyd H, Emanuelsson C, Finet S, Golenhofen N, Goloubinoff P, Gusev N, Haslebeck M, Hightower LE, Kampinga HH, Klevit RE, Liberek K, Mchaourab HS, McMenimen KA, Poletti A, Quinlan R, Strelkov SV, Toth ME, Vierling E, Tanguay RM, The growing world of small heat shock proteins: from structure to functions, Cell Stress Chaperones 22 (2017) 601–611. [PubMed: 28364346]

[5]. Itakura E, Chiba M, Murata T, Matsuura A, Heparan sulfate is a clearance receptor for aberrant extracellular proteins, J. Cell Biol 219 (2020), e201911126, 10.1083/jcb.201911126. [PubMed: 32211892]

[6]. Benson MD, Buxbaum JN, Eisenberg DS, Merlini G, Saraiva MJM, Sekijima Y, Sipe JD, Westermark P, Amyloid nomenclature 2018: recommendations by the International Society of Amyloidosis (ISA) nomenclature committee, Amyloid 25 (2018) 215–219. [PubMed: 30614283]

[7]. Walsh DM, Klyubin I, Fadeeva JV, Cullen WK, Anwyl R, Wolfe MS, Rowan MJ, Selkoe DJ, Naturally secreted oligomers of amyloid beta protein potently inhibit hippocampal long-term potentiation in vivo, Nature 416 (2002) 535–539. [PubMed: 11932745]

[8]. Buxbaum J, Johansson J, Transthyretin and BRICHOS: the paradox of amyloidogenic proteins with anti-amyloidogenic activity for aβ in the central nervous system, Front. Neurosci 11 (2017) 119, 10.3389/fnins.2017.00119. [PubMed: 28360830]

[9]. Willander H, Askarieh G, Landreh M, Westermark P, Nordling K, Keränen H, Hermansson E, Hamvas A, Nogee LM, Bergman T, Saenz A, Casals C, Åqvist J, Jörnvall H, Berglund H, Presto J, Knight SD, Johansson J, High-resolution structure of a BRICHOS domain and its implications for anti-amyloid chaperone activity on lung surfactant protein C, Proc. Natl. Acad. Sci. U. S. A 109 (2012) 2325–2329. [PubMed: 22308375]

[10]. Oskarsson ME, Hermansson E, Wang Y, Welsh N, Presto J, Johansson J, Westermark GT, BRICHOS domain of Bri2 inhibits islet amyloid polypeptide (IAPP) fibril formation and toxicity in human beta-cells, Proc. Natl. Acad. Sci. U. S. A 115 (2018) E2752–E2761. [PubMed: 29507232]

[11]. Vidal R, Frangione B, Rostagno A, Mead S, Révész T, Plant G, Ghiso J, A stop-codon mutation in the BRI gene associated with familial British dementia, Nature 399 (1999) 776–781. [PubMed: 10391242]

[12]. Chen G, Abelein A, Nilsson HE, Leppert A, Andrade-Talavera Y, Tambaro S, Hemmingsson L, Roshan F, Landreh M, Biverstål H, Koeck PJB, Presto J, Hebert H, Fisahn A, Johansson J, Bri2 BRICHOS client specificity and chaperone activity are governed by assembly state, Nat. Commun 8 (2017) 2081. [PubMed: 29234026]

[13]. Chen G, Andrade-Talavera Y, Tambaro S, Leppert A, Nilsson HE, Zhong X, Landreh M, Nilsson P, Hebert H, Biverstål H, Fisahn A, Abelein A, Johansson J, Augmentation of Bri2 molecular chaperone activity against amyloid-β reduces neurotoxicity in mouse hippocampus in vitro, Commun. Biol 3 (2020) 32, 10.1038/s42003-020-0757-z. [PubMed: 31959875]

[14]. Cohen SIA, Arosio P, Presto J, Kurudenkandy FR, Biverstål H, Dolfe L, Dunning C, Yang X, Frohm B, Vendruscolo M, Johansson J, Dobson CM, Fisahn A, Knowles TPJ, Linse S, A molecular chaperone breaks the catalytic cycle that generates toxic Aβ oligomers, Nat. Struct. Mol. Biol 22 (2015) 207–213. [PubMed: 25686087]

[15]. Poska H, Haslbeck M, Kurudenkandy FR, Hermansson E, Chen G, Kostallas G, Abelein A, Biverstål H, Crux S, Fisahn A, Presto J, Johansson J, Dementia-related Bri2 BRICHOS is a versatile molecular chaperone that efficiently inhibits Aβ42 toxicity in Drosophila, Biochem. J 473 (2016) 3683–3704. [PubMed: 27514716]

[16]. Martins F, Marafona AM, Pereira CD, Müller T, Loosse C, Kolbe K, da Cruz e Silva OAB, Rebelo S, Identification and characterization of the BRI2 interactome in the brain, Sci. Rep 8 (2018) 3548, 10.1038/s41598-018-21453-3. [PubMed: 29476059]

[17]. Moaddel R, Marszałł MP, Bighi F, Yang Q, Duan X, Wainer IW, Automated ligand fishing using human serum albumin-coated magnetic beads, Anal. Chem 79 (2007) 5414–5417. [PubMed: 17579480]

[18]. Yasuda M, Wilson DR, Fugmann SD, Moaddel R, Synthesis and characterization of SIRT6 protein coated magnetic beads: identification of a novel inhibitor of SIRT6 deacetylase from medicinal plant extracts, Anal. Chem 83 (2011) 7400–7407. [PubMed: 21854049]

[19]. Marszall MP, Moaddel R, Kole S, Gandhari M, Bernier M, Wainer IW, Ligand and protein fishing with heat shock protein 90 coated magnetic beads, Anal. Chem 80 (2008) 7571–7575. [PubMed: 18693748]

[20]. Kronqvist N, Sarr M, Lindqvist A, Nordling K, Otikovs M, Venturi L, Pioselli B, Purhonen P, Landreh M, Biverstål H, Toleikis Z, Sjöberg L, Robinson CV, Pelizzi N, Jörnvall H, Hebert H,

Jaudzems K, Curstedt T, Rising A, Johansson J, Efficient protein production inspired by how spiders make silk, Nat. Commun 8 (2017) 15504. [PubMed: 28534479]

[21]. Poska H, Leppert A, Tigro H, Zhong X, Kaldmäe M, Nilsson HE, Hebert H, Chen G, Johansson J, Recombinant Bri3 BRICHOS domain is a molecular chaperone with effect against amyloid formation and non-fibrillar protein aggregation, Sci. Rep 10 (2020) 9817, 10.1038/s41598-020-66718-y. [PubMed: 32555390]

[22]. Walsh DM, Thulin E, Minogue AM, Gustavsson N, Pang E, Teplow DB, Linse S, A facile method for expression and purification of the Alzheimer's disease-associated amyloid β-peptide, FEBS J. 276 (2009) 1266–1281. [PubMed: 19175671]

[23]. Ubaida-Mohien C, Gonzalez-Freire M, Lyashkov A, Moaddel R, Chia CW, Simonsick EM, Sen R, Ferrucci L, Physical activity associated proteomics of skeletal muscle: being physically active in daily life may protect skeletal muscle from aging, Front. Physiol 10 (2019) 312, 10.3389/fphys.2019.00312. [PubMed: 30971946]

[24]. Knight SD, Presto J, Linse S, Johansson J, The BRICHOS domain, amyloid fibril formation, and their relationship, Biochemistry 52 (2013) 7523–7531. [PubMed: 24099305]

[25]. Del Campo M, Oliveira CR, Scheper W, Zwart R, Korth C, Müller-Schiffmann A, Kostallas G, Biverstål H, Presto J, Johansson J, Hoozemans JJ, Pereira CF, Teunissen CE, BRI2 ectodomain affects Aβ42 fibrillation and tau truncation in human neuroblastoma cells, Cell. Mol. Life Sci 72 (2015) 1599–1611. [PubMed: 25336154]

[26]. Butterfield DA, Hardas SS, Lange MLB, Oxidatively modified Glyceraldehyde-3-Phosphate dehydrogenase (GAPDH) and alzheimer disease: many pathways to neurodegeneration, J. Alzheimers Dis 20 (2010) 369–393. [PubMed: 20164570]

[27]. Leppert A, Tiiman A, Kronqvist N, Landreh M, Abelein A, Vukojevic V, Johansson J, Smallest secondary nucleation competent Aβ aggregates probed by an ATP-independent molecular chaperone domain, Biochemistry (2021), 10.1021/acs.biochem.1c00003, In press.

[28]. Tolias KF, Duman JG, Um K, Control of synapse development and plasticity by Rho GTPase regulatory proteins, Prog. Neurobiol 94 (2011) 133–148. [PubMed: 21530608]

[29]. Miller DJ, Fort PE, Heat shock proteins regulatory role in Neurodevelopment, Front. Neurosci 12 (2018) 821, 10.3389/fnins.2018.00821. [PubMed: 30483047]

[30]. Karunanithi S, Brown IR, Heat shock response and homeostatic plasticity, Front. Cell. Neurosci 9 (2015) 68, 10.3389/fncel.2015.00068. [PubMed: 25814928]

[31]. Aguilar BJ, Zhu Y, Lu Q, Rho GTPases as therapeutic targets in Alzheimer's disease, Alzheimers Res. Ther 9 (2017) 97, 10.1186/s13195-017-0320-4. [PubMed: 29246246]

[32]. Ciavardelli D, Silvestri E, Del Viscovo A, Bomba M, De Gregorio D, Moreno M, Di Ilio C, Goglia F, Canzoniero LMT, Sensi SL, Alterations of brain and cerebellar proteomes linked to Aβ and tau pathology in a female triple-transgenic murine model of Alzheimer's disease, Cell Death Dis. 1 (2010) e90, 10.1038/cddis.2010.68. [PubMed: 21368863]

[33]. Willander H, Hermansson E, Johansson J, Presto J, BRICHOS domain associated with lung fibrosis, dementia and cancer – a chaperone that prevents amyloid fibril formation? FEBS J. 278 (2011) 3893–3904. [PubMed: 21668643]

[34]. Dolfe L, Tambaro S, Tigro H, Del Campo M, Hoozemans JJM, Wiehager B, Graff C, Winblad B, Ankarcrona M, Kaldmäe M, Teunissen CE, Rönnbäck A, Johansson J, Presto J, The Bri_2 and Bri3 BRICHOS domains interact differently with $A\beta_{42}$ and alzheimer amyloid plaques, J. Alzheimers Dis. Rep 2 (2018) 27–39. [PubMed: 30480246]

[35]. Itakura M, Nakajima H, Kubo T, Semi Y, Kume S, Higashida S, Kaneshige A, Kuwamura M, Harada N, Kita A, Azuma Y-T, Yamaji R, Inui T, Takeuchi T, Glyceraldehyde-3-phosphate dehydrogenase aggregates accelerate Amyloid-β amyloidogenesis in alzheimer disease, J. Biol. Chem 290 (2015) 26072–26087. [PubMed: 26359500]

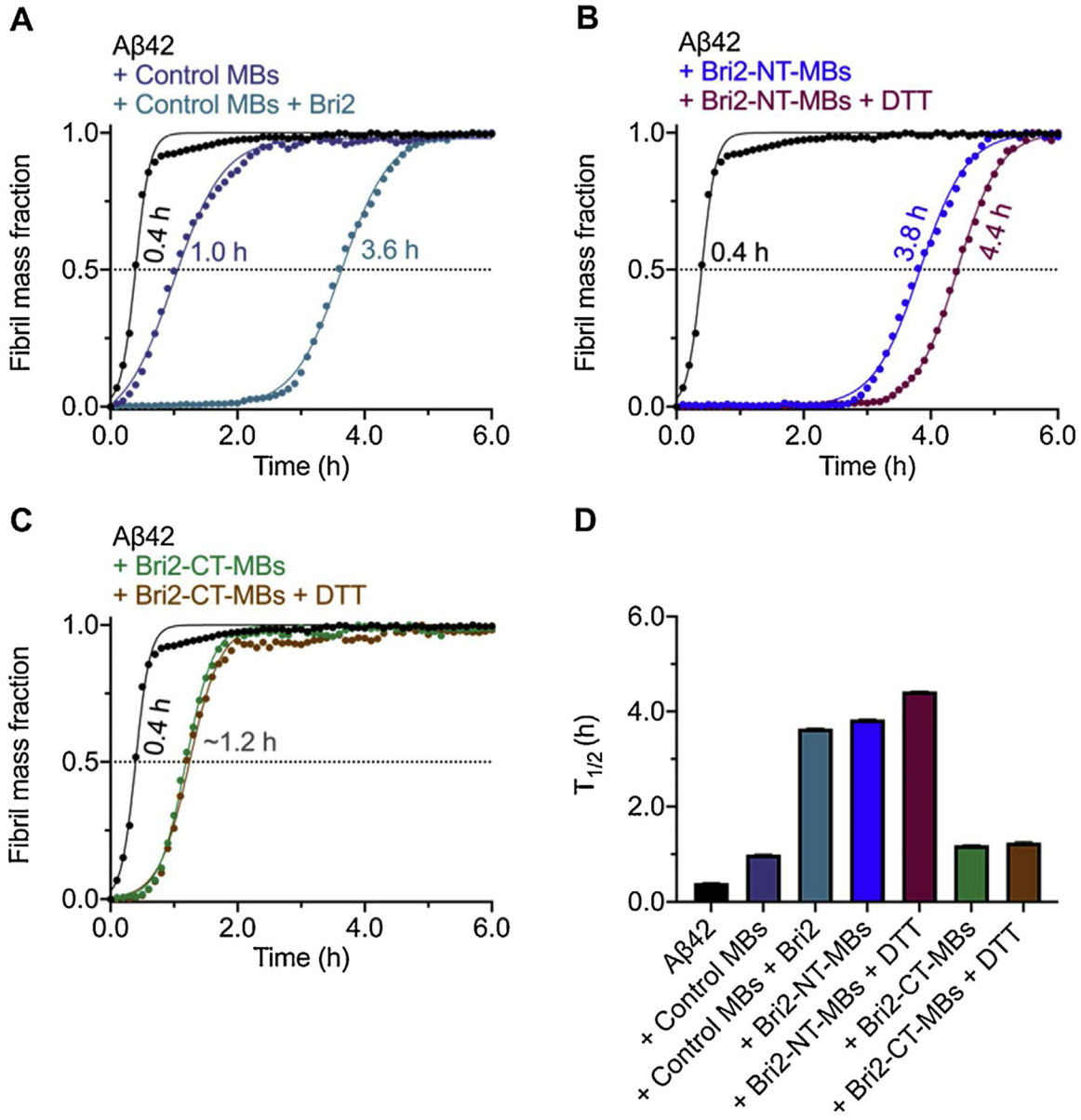

Fig. 1.

Kinetic analysis of Aβ42 in the absence and presence of Bri2-NT-MB, Bri2-CT-M and Control-MB with and without rh Bri2 BRICHOS on Aβ42 fibril formation measured by ThT fluorescence.

The data presented shows the kinetic analysis of fibril formation of 3 μM Aβ42 alone and with **A**. Control-MBs only and Control-MBs with 3 μM rh Bri2 BRICHOS domain; **B**. Bri2-NT-MB only and Bri2-NT-MB with 0.1 mM DTT; **C**. Bri2-CT-MB only and Bri2-CT-MB with 0.1 mM DTT. **D**. shows direct $T_{1/2}$ (h) comparison from A, B and C. The measurements were done in quadruplicate and individual sigmoidal fits (solid lines) of normalized and averaged aggregation traces (dots) are presented.

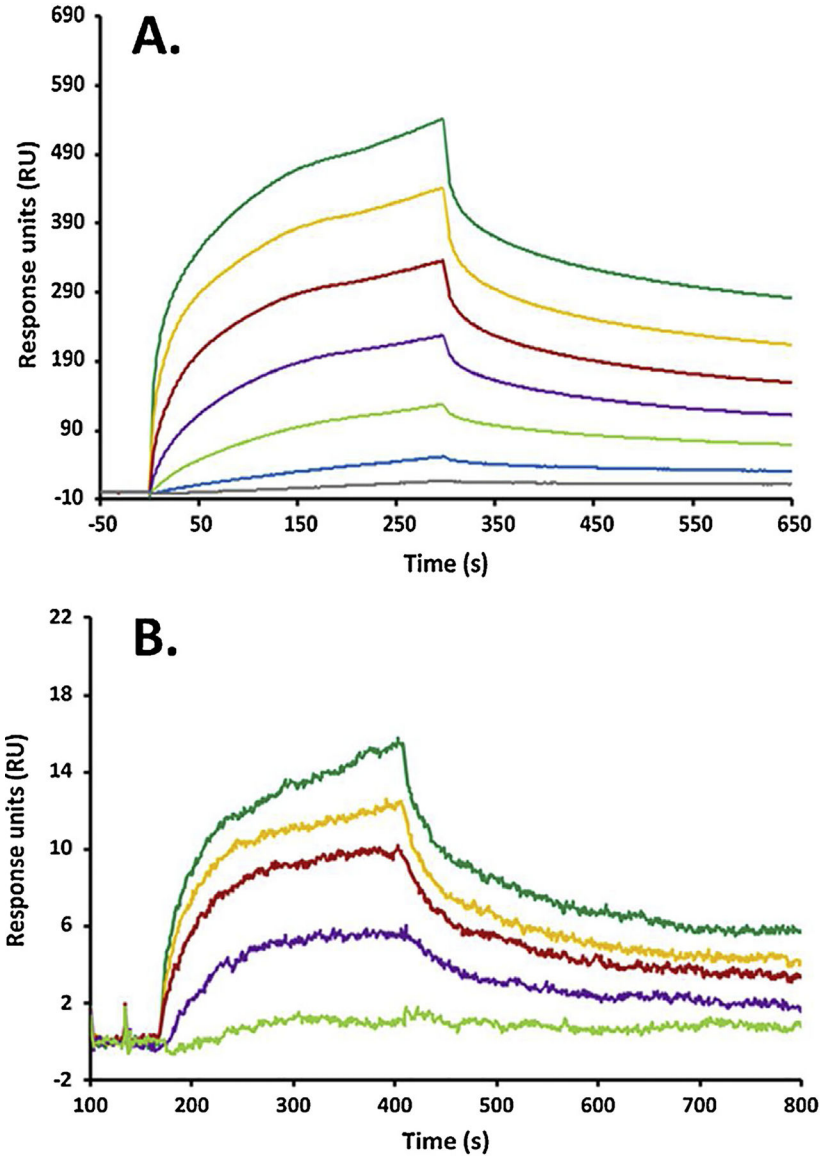

Fig. 2.

SPR analysis of ApoA1 and GAPDH binding to immobilized Bri2 BRICHOS.Crude rh Bri2 BRICHOS was immobilized to a sensor chip by amine coupling. SPR sensorgrams were recorded at **A**. seven different GAPDH tetramer concentrations: 2.5 μM (dark green), 1.3 μM (yellow), 0.63 μM (red), 0.31 μM (purple), 0.16 μM (light green), 0.078 μM (blue) and 0.039 μM (grey) and **B**. five different Apo-A1 monomer concentrations: 17.7 μM (dark green), 8.8 μM (yellow), 4.4 μM (red), 2.2 μM (purple) and 1.1 μM (light green) injected over the chip surface.

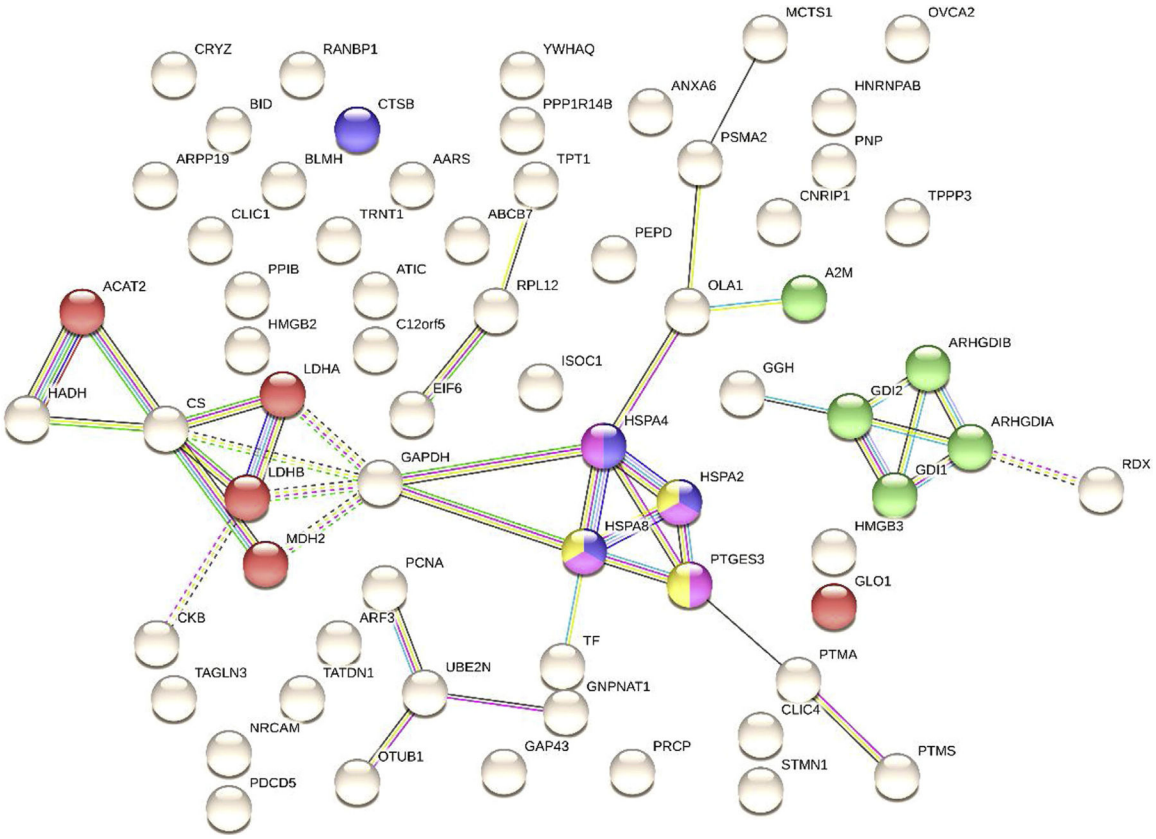

Fig. 3.

Enrichment Analysis of interacting proteins with Bri2 BRICHOS. STRING analysis was carried out on proteins that were significantly increased in the Elute 2 fraction of the Bri2-NT-MB Proteins relative to the Control-MB. Identified pathways including pyruvate and cysteine and methionine metabolism (red), Reactome pathways: Rho GTPase cycle (green) and cellular response heat stress (blue). STRING analysis was performed with high confidence (0.7), and significant reactome and KEGG pathways correspond to FDR < 0.05. The protein network metrics are: Number of nodes: 89; number of edges:70; average node degree: 1.57; average local clustering coefficient: 0.329; expected number of edges: 26; PPI enrichment p-value: 9.92e-13.

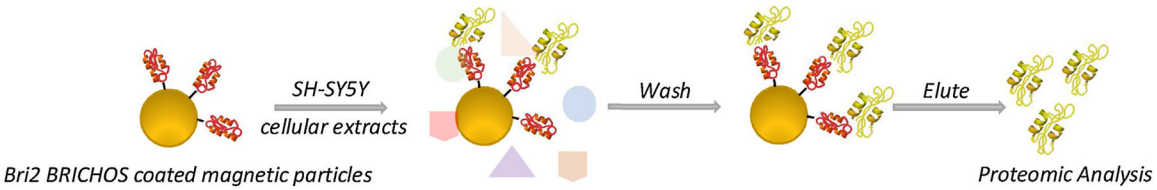

Scheme 1.

Flow chart for protein fishing experiments carried out in SH-SY5Y cellular extracts using Bri2 BRICHOS coated magnetic beads.

Table 1

The proteins that were removed from the Bri2-NT-MB and Control-MBs incubated in the cytosolic fraction of cell homogenates of SH-SY5Y cells, following two washes with 1x PBS, an elution with 10 μM rh Bri2 BRICHOS and an incubation with 1X PBS at room temperature. The difference in spectral counts between the Bri2-NT-MBs and Control-MBs (Δ) is reported and the statistical significance (p-value <0.025) and those reported with p-values between 0.025 and 0.050 are reported in Supplemental Table 1.

Protein Hits	Δ	p-value
Ran-specific GTPase-activating protein **RANBP1**	9.67	0.000
High mobility group protein B3 **HMGB3**	8.33	0.002
Rho GDP-dissociation inhibitor 1 **ARHGDIA**	29.67	0.002
L-lactate dehydrogenase B chain **LDHB**	17.00	0.004
Citrate synthase, mitochondrial **CS**	10.67	0.004
Ubiquitin thioesterase **OTUB1**	8.33	0.006
Parathymosin **PTMS**	49.67	0.007
Rab GDP dissociation inhibitor alpha **GDI1**	48.00	0.007
Ubiquitin-conjugating enzyme E2 N **UBE2N**	6.67	0.008
Translationally-controlled tumor protein **TPT1**	10.67	0.010
Ovarian cancer-associated gene 2 protein **OVCA2**	3.33	0.010
Protein phosphatase 1 regulatory subunit 14B **PPP1R14B**	7.33	0.010
Lysosomal Pro-X carboxypeptidase **PRCP**	3.33	0.013
Gamma-glutamyl hydrolase **GGH**	3.33	0.013
Lactoylglutathione lyase **GLO1**	3.33	0.013
Acetyl-CoA acetyltransferase, cytosolic **ACAT2**	9.33	0.013
Hydroxyacyl-coenzyme A dehydrogenase, mitochondrial **HADH**	4.00	0.013
Chloride intracellular channel protein 1 **CLIC1**	16.67	0.014
Programmed cell death protein 5 **PDCD5**	3.67	0.015
Purine nucleoside phosphorylase **PNP**	12.67	0.015
Rho GDP-dissociation inhibitor 2 **ARHGDIB**	8.00	0.015
RNA 3′-terminal phosphate cyclase **RTCA**	2.67	0.015
Neuromodulin **GAP43**	4.67	0.016
Malignant T-cell-amplified sequence 1 **MCTS1**	6.33	0.019
Transgelin-3 **TAGLN3**	5.00	0.019
Prosaposin **PSAP**	2.33	0.020
Glycine cleavage system H protein, mitochondrial **GCSH**	2.33	0.020
Heterogeneous nuclear ribonucleoprotein A/B **HNRNPAB**	4.00	0.020
Tubulin polymerization-promoting protein family member 3 **TPPP3**	4.00	0.020
cAMP-regulated phosphoprotein 19 **ARPP19**	9.33	0.022
BH3-interacting domain death agonist **BID**	3.33	0.022
Eukaryotic translation initiation factor 6 **EIF6**	10.00	0.023
Prothymosin alpha **PTMA**	55.33	0.024
Bleomycin hydrolase **BLMH**	10.33	0.024
Neuronal cell adhesion molecule **NRCAM**	25.00	0.025